



ISTITUTO NAZIONALE DI FISICA NUCLEARE - ISTITUTO NAZIONALE DI FISICA NUCLEARE - ISTITUTO NAZIONALE DI FISICA NUCLEARE - ISTITUTO NAZIONALE DI FISICA NUCLEARE

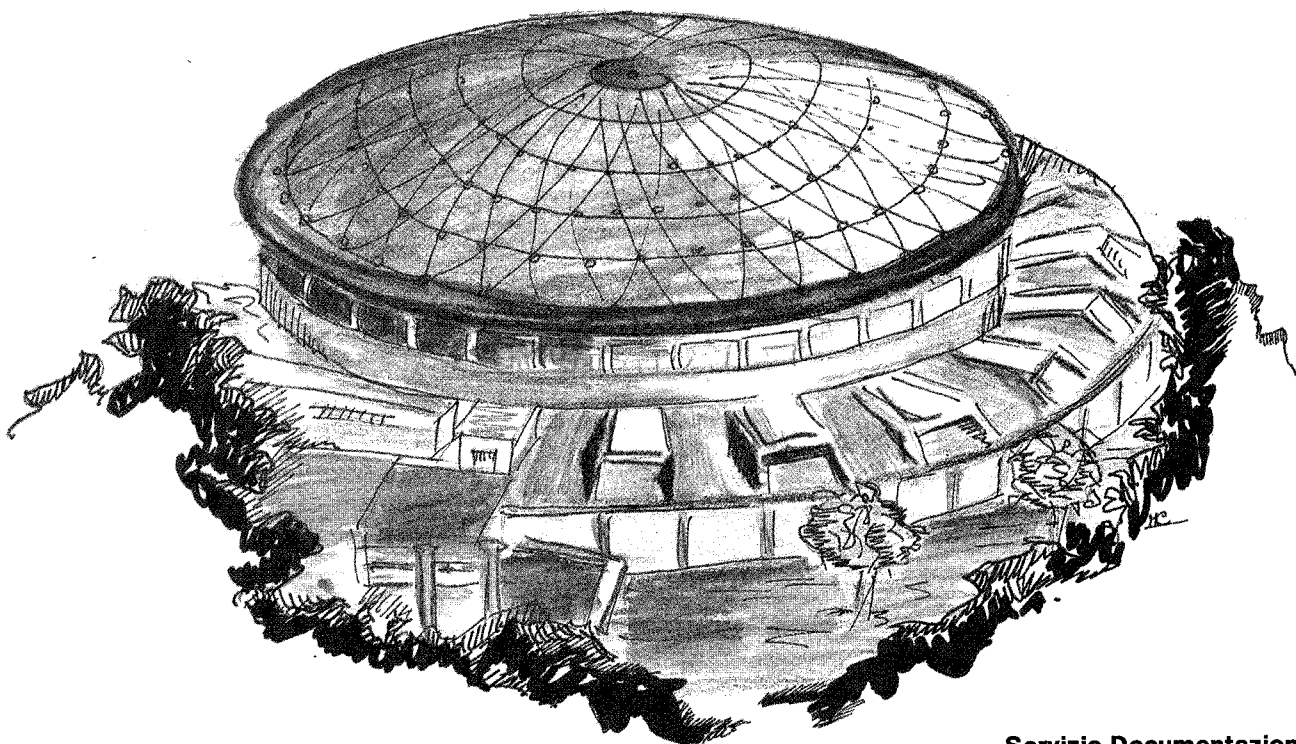
Laboratori Nazionali di Frascati

Submitted to Phys. Lett.

LNF-90/0048(PT)
7 Giugno 1990

A. Grau, G. Pancheri, Y.N. Srivastava:

CONTRIBUTION OF QUARK-ANTIQUARK ANNIHILATION TO THE PRODUCTION OF VIRTUAL Z_0 -PAIRS IN HADRON COLLISIONS



Servizio Documentazione
dei Laboratori Nazionali di Frascati
P.O. Box, 13 - 00044 Frascati (Italy)

INFN - Laboratori Nazionali di Frascati
Servizio Documentazione

LNF-90/048(PT)
7 Giugno 1990

**Contribution of Quark-antiquark Annihilation
to the Production of Virtual Z_0 -pairs in Hadron Collisions**

A. Grau

Universitat Autònoma de Barcelona, 08193 Bellaterra, Spain

G. Pancheri

Physics Department, Universita' di Palermo, Palermo, Italy
and

INFN, Laboratori Nazionali di Frascati, P.O.Box 13, 00044 Frascati, Italy

and

Y.N.Srivastava

INFN, University of Perugia, Perugia, Italy

Abstract

We calculate the contribution of quark-antiquark annihilation to the production of virtual Z_0 -pairs in hadron colliders like LHC or SSC. This process can constitute a potentially important background to the detection of an intermediate Higgs boson, i.e. $M_Z \leq M_H \leq 2M_Z$. We show that this cross-section is always one or more orders of magnitude smaller than the signal, provided a resolution of at least 10 GeV in the invariant mass of the Z_0 pairs is available. The signal for different values of the top mass is compared with the background cross-section at two c.m. energies , 16, and 40 TeV .

Recent measurements in e^+e^- annihilation^[1] have established that the Higgs boson mass cannot be less than 24 GeV. This limit is expected to be raised to as much as 70-80 GeV in the years to come, when LEP-200 will start operating^[2]. The search for Higgs in the higher mass range will then be left to the hadron colliders. This range can be roughly divided into two main regimes : one in which the Higgs boson is lighter than two Vector Bosons(IVB's) and one in which it is heavier. The limits recently imposed on the top mass by the CDF collaboration^[3], have now established that the heaviest quark below the W-mass is the bottom quark, so that the two regions differ because the dominant Higgs decay mode in one case will be into $b\bar{b}$ pairs and in the other into a pair of IVB's. The hadronic backgrounds, however, are so overwhelming that the search for the Higgs boson , in either regions, may have to focus on the leptonic decay channels^[4], i.e. $H \rightarrow \gamma\gamma$ or

$$H \rightarrow Z_0 Z_0 \rightarrow 2l^+ 2l^- \quad (1)$$

where l^\pm stands for either electrons or μ 's. Notice that, in what follows , we shall consider $l = \mu$: if both electrons and muons can be detected, all the relevant quantities can be multiplied by a factor 4.

One of the possible background processes is constituted by Z_0 -pairs of QCD origin. In the region above the two IVB threshold this background has been extensively studied and shown to be well below the signal^[5] until $M_H \leq 700$ GeV at the LHC/SSC. On the other hand, the studies of this background in the lower region, the so called "intermediate Higgs" regime, are not yet complete. In this region, we have background contributions from the following processes :

$$q\bar{q} \rightarrow Z_0^* Z_0^* \rightarrow (\mu^+ \mu^-)(\mu^+ \mu^-) \quad (2)$$

$$q\bar{q} \rightarrow Z_0^* \gamma^* \rightarrow (\mu^+ \mu^-)(\mu^+ \mu^-) \quad (3)$$

and

$$gg \rightarrow Z_0^* Z_0^* \rightarrow (\mu^+ \mu^-)(\mu^+ \mu^-) \quad (4)$$

or

$$gg \rightarrow Z_0^* \gamma^* \rightarrow (\mu^+ \mu^-)(\mu^+ \mu^-) \quad (5)$$

Although processes (4) and (5) are of higher order in the strong coupling constant α_s , the large gluon densities in the x-values of interest make these processes comparable in magnitude to $q\bar{q}$ annihilation. In other words, the logarithmic growth in the gluon densities compensates for the (inverse) logarithmic behaviour in α_s . Recent calculations by Glover et al. for the case in which the two Z_0 's are real have shown that the gluon-gluon processes contribute as much as 50-70 % of the $q\bar{q}$ processes, in the collider energy region of interest. One can expect this to remain approximately true also for production of Z-pairs below threshold, i.e. for processes

(2) and (4), although as the Higgs mass decreases, the production of gluons over that of quarks is bound to increase further. While work is in progress to estimate the contribution of processes (4) and (5) to production of 4μ 's from real and virtual Z_0 's, in what follows we shall study the cross section for the process

$$pp \rightarrow q\bar{q} + X \rightarrow Z_0^* Z_0^* + X \rightarrow (\mu^+ \mu^-)(\mu^+ \mu^-) + X \quad (6)$$

The parton-parton subprocess receives contribution from the two graphs of fig.1. The cross-section can be written as

$$\begin{aligned} d\hat{\sigma} &= \frac{1}{2\hat{s}} \frac{1}{(2\pi)^8} \sum |M|^2 dPS(ab \rightarrow p_1 + p_2 + p_3 + p_4) = \\ &= \frac{1}{24} \frac{1}{2\hat{s}} \frac{1}{(2\pi)^8} \sum |M|^2 d^2PS(a+b \rightarrow (12) + (34)) \\ &\quad dQ_1^2 dQ_2^2 d^2PS(Q_1 \rightarrow p_1 + p_2) d^2PS(Q_2 \rightarrow p_3 + p_4) \theta(\sqrt{\hat{s}} - Q_1 - Q_2) \end{aligned} \quad (7)$$

where the factor $\frac{1}{24}$ comes from averaging over initial color and spin and symmetrizing over the two Z_0^* in the final state. In the above expression, the four-body phase space has been factorized into a sequence of two-body phase space factors while the θ function ensures energy conservation for any given parton-parton c.m. energy $\sqrt{\hat{s}}$. The squared matrix element $|M|^2$ is given by

$$|M|^2 = \frac{g^4}{\cos^4\theta_W} \frac{\text{Tr} [\not{a}(V - A\gamma_5)t^{\mu\lambda} \not{b}t^{\sigma\nu}(V + A\gamma_5)] \text{Tr} [G_{\mu\sigma}(12)] \text{Tr} [G_{\lambda\nu}(34)]}{D_1 D_2}$$

where

$$V = (g_V^f)^2 + (g_A^f)^2 \quad A = 2g_A^f g_V^f$$

with g_V and g_A the usual coupling of the Z_0 -boson to the fermions. For massless fermions, we also have

$$t_{\mu\lambda} = \gamma_\mu \frac{\not{q}}{q^2} \gamma_\lambda + \gamma_\lambda \frac{\not{p}}{p^2} \gamma_\mu$$

and

$$G_{\mu\sigma}(12) = \not{p}_1 \gamma_\lambda \Gamma_f \not{p}_2 \Gamma_f^\dagger \gamma_\sigma$$

with

$$\Gamma_f = -i \frac{g}{\cos\theta_W} (g_V^f + g_A^f \gamma_5)$$

with the index f to indicate the particular fermion pair into which each real or virtual Z_0 will decay. The denominators D_1 and D_2 represent the Z_0 propagators, i.e.

$$D_i = (Q_i^2 - m_Z^2)^2 + m_Z^2 \Gamma_Z^2$$

The calculation is straightforward and similar to the one in which the Z_0 are real, except that one must keep track of the different masses Q_1^2 and Q_2^2 . Upon performing phase space integration , and redefinig

$$g_V = \frac{1}{2}(g_R + g_L), \quad g_A = \frac{1}{2}(g_R - g_L)$$

the cross section becomes

$$\begin{aligned} d^3\hat{\sigma} &= \int_{4body LIPS} d\hat{\sigma} = \\ &\frac{\pi p^*}{\hat{s}\sqrt{\hat{s}}} \frac{dz^*}{6} \left(\frac{m_Z \Gamma_Z}{\pi} \right)^2 \frac{dQ_1^2}{(Q_1^2 - m_Z^2)^2 + m_Z^2 \Gamma_Z^2} \frac{dQ_2^2}{(Q_2^2 - m_Z^2)^2 + m_Z^2 \Gamma_Z^2} \\ &\left(\frac{\Gamma_{Z \rightarrow \mu^+ \mu^-}}{\Gamma_Z} \right)^2 \frac{\alpha^2}{x_W^2 (1 - x_W)^2} (g_L^4 + g_R^4) \frac{Q_1^2 Q_2^2}{m_Z^4} B(\hat{s}, \hat{t}, \hat{u}) \end{aligned} \quad (8)$$

with

$$B(\hat{s}, \hat{t}, \hat{u}) = -Q_1^2 Q_2^2 \left(\frac{1}{\hat{t}^2} + \frac{1}{\hat{u}^2} \right) + \frac{\hat{u}}{\hat{t}} + \frac{\hat{t}}{\hat{u}} + \frac{2\hat{s}(Q_1^2 + Q_2^2)}{\hat{u}\hat{t}}$$

where the invariants of the parton-parton subprocess are given by

$$\hat{t} = Q_1^2 - \sqrt{\hat{s}}E_1 + p^*\sqrt{\hat{s}}z^*$$

$$\hat{u} = Q_1^2 - \sqrt{\hat{s}}E_1 - p^*\sqrt{\hat{s}}z^*$$

and $z^* = \cos\theta^*$ with θ^* the parton-parton center of mass scattering angle. In the above equation , E_1 is the energy of one of the two Z_0 , which is given by

$$E_1 = \frac{\hat{s} + Q_1^2 - Q_2^2}{2\sqrt{\hat{s}}}$$

and p^* is the center of mass momentum of the final IVB's. It is easy to see that, in the narrow width approximation, the above expression reduces to the known one for production of two real Z_0 's. One can also check that if one of two Z_0 's is on the mass shell, our expression concides with the one obtained by Gunion, Kalyniak, Soldate and Galison^[6]. To check it is necessary to integrate the expression obtained by these authors over the invariant phase space of the two fermions into which the virtual Z_0 decays. The result of this integration shows that the function $B(\hat{s}, \hat{t}, \hat{u})$ is replaced by

Erratum: LNF-90/0048(PT)

A. Grau

Universitat Autònoma de Barcelona, 08193 Bellaterra, Spain

G. Pancheri

Physics Department, Universita' di Palermo, Palermo, Italy
and

INFN, Laboratori Nazionali di Frascati, P.O.Box 13, 00044 Frascati, Italy

Y.N.Srivastava

INFN, University of Perugia, Perugia, Italy

Eq.(10) should be substituted by :

$$\int_{-z_1}^{z_0} B(\hat{s}, \hat{t}, \hat{u}) = -2Q_1^2 Q_2^2 \left[\frac{z_0}{(\sqrt{\hat{s}}E_1 - Q_1^2)^2 - \hat{s}p^{*2}z_0^2} + \frac{z_1}{(\sqrt{\hat{s}}E_1 - Q_1^2)^2 - \hat{s}p^{*2}z_1^2} \right] - \\ -2(z_0 + z_1) + \frac{1}{\sqrt{\hat{s}}p^*} \left[2(\sqrt{\hat{s}}E_1 - Q_1^2) + \frac{\hat{s}(Q_1^2 + Q_2^2)}{\sqrt{\hat{s}}E_1 - Q_1^2} \right] \cdot \\ \cdot \left[\ln \frac{\sqrt{\hat{s}}E_1 - Q_1^2 + \sqrt{\hat{s}}p^*z_1}{\sqrt{\hat{s}}E_1 - Q_1^2 - \sqrt{\hat{s}}p^*z_0} + \ln \frac{\sqrt{\hat{s}}E_1 - Q_1^2 + \sqrt{\hat{s}}p^*z_0}{\sqrt{\hat{s}}E_1 - Q_1^2 - \sqrt{\hat{s}}p^*z_1} \right]$$

where

$$z_1 = \min [1, \beta_2^{-1} \tanh(y_{cut} - |y|), \beta_1^{-1} \tanh(y_{cut} + |y|)],$$

$$z_0 = \min [1, \beta_1^{-1} \tanh(y_{cut} - |y|)], \quad \text{for } |y_Z| \text{ or } |y_H| \leq y_{cut}$$

and

$$\beta_1 = \frac{p^*}{E_1}, \quad \beta_2 = \frac{p^*}{E_2}$$

The numerical results remain unchanged.

$$B'(\hat{s}, \hat{t}, \hat{u}) = -m_Z^2 s_H \left(\frac{1}{\hat{t}^2} + \frac{1}{\hat{u}^2} \right) + \frac{\hat{u}}{\hat{t}} + \frac{\hat{t}}{\hat{u}} + \frac{2\hat{s}(m_Z^2 + s_H)}{\hat{u}\hat{t}}$$

which is precisely what one would obtain, by performing the narrow width approximation for one of the two Z_0 's.

We can obtain the hadronic cross-section for process (1) by folding the parton-parton cross-section of eq.(8) with the parton densities. The cross-section then becomes

$$\begin{aligned} \frac{d\sigma(pp \rightarrow q\bar{q} + X \rightarrow Z_0^* Z_0^* + X \rightarrow 4\mu + X)}{dM dQ_1 dQ_2 dy} &= \\ \sum_i (g_{Li}^4 + g_{Ri}^4) F_i(\sqrt{\tau} e^y, M^2) F_{\bar{i}}(\sqrt{\tau} e^{-y}, M^2) & \\ \frac{4\pi p^*}{3M^4} \frac{\alpha^2}{x_W^2(1-x_W)^2} (B_{Z \rightarrow \mu^+ \mu^-})^2 \frac{Q_1^3 Q_2^3}{m_Z^4} \left(\frac{m_Z \Gamma_Z}{\pi} \right)^2 \frac{1}{D_1 D_2} \int_{-z_0}^{z_0} B(\hat{s}, \hat{t}, \hat{u}) & \end{aligned} \quad (9)$$

The integration over the scattering angle gives

$$\begin{aligned} \int_{-z_0}^{z_0} B(\hat{s}, \hat{t}, \hat{u}) &= -4z_0 + \frac{2}{\sqrt{\hat{s}p^*}} \left[2 \left(\sqrt{\hat{s}} E_1 - Q_1^2 \right) + \frac{\hat{s}(Q_1^2 + Q_2^2)}{\sqrt{\hat{s}} E_1 - Q_1^2} \right] \\ &\log \frac{\sqrt{\hat{s}} E_1 - Q_1^2 + \sqrt{\hat{s}p^*} z_0}{\sqrt{\hat{s}} E_1 - Q_1^2 - \sqrt{\hat{s}p^*} z_0} \\ &- \frac{4Q_1^2 Q_2^2 z_0}{(\sqrt{\hat{s}} E_1 - Q_1^2)^2 - \hat{s}p^{*2} z_0^2} \end{aligned} \quad (10)$$

This expression should be directly compared with the one which describes the same final state as obtained from gluon-gluon fusion into a Higgs boson. Before discussing the phenomenological applications of our expression, lets us in fact list the one to be used for the signal. We shall then examine these two, first separately, and then together.

The cross section for the process of fig.2 can be written as

$$\begin{aligned} \frac{d\sigma(pp \rightarrow gg + X \rightarrow H + X \rightarrow 4\mu + X)}{dM dQ_1 dQ_2 dy} &= MG(\sqrt{\tau} e^y, M_H^2) G(\sqrt{\tau} e^{-y}, M_H^2) \frac{G_F \pi}{16\sqrt{2}} \\ \left(\frac{\alpha_s}{\pi} \right)^2 |\eta_{gg}|^2 \frac{M_H \Gamma_H}{\pi D_H} \frac{p^*}{\Gamma_H} \frac{G_F}{8\pi\sqrt{2}} \frac{Q_1^3 Q_2^3}{M_H^2 D_1 D_2} \left(\frac{\Gamma_Z m_Z}{\pi} \right)^2 (B_{Z \rightarrow \mu^+ \mu^-})^2 C(Q_1^2, Q_2^2, M^2) & \end{aligned} \quad (11)$$

where

$$C(Q_1^2, Q_2^2, M^2) = 4 \frac{2Q_1^2 Q_2^2 + (Q_1 \cdot Q_2)^2}{Q_1^2 Q_2^2}$$

In eq.(11) the factor $C(Q_1^2, Q_2^2, M^2)$ is the analogue of factor $B(\hat{s}, \hat{t}, \hat{u})$ of eq.(10), $|\eta_{gg}|^2$ is the usual integral over the triangle diagram, i.e. such that

$$\Gamma(H \rightarrow gluon\ gluon) = \frac{G_F M_H^3}{4\pi\sqrt{s}} \left[\frac{\alpha_s(M_H^2)}{\pi} \right]^2 |\eta_{gg}|^2$$

Also

$$D_H = (M^2 - M_H^2)^2 + M_H^2 \Gamma_H^2$$

In the region where the Z_0 's are off the mass shell (generally only one of them, if $M_H \geq m_Z$), the Higgs boson is extremely narrow, and one can very well use the narrow width approximation to estimate the cross-section. On the other hand, above the two IVB threshold, the Higgs has an increasingly large width and it is necessary to keep the propagator. In this region however the two Z_0 's are on the mass shell and one can use the delta function approximation for the Z_0 propagators. We show in Fig.3 the Higgs boson production cross section and subsequent decay into 4μ 's in the region below and around the two Z_0 's threshold, for different values of the top mass, at the energy $\sqrt{s} = 16\text{TeV}$. We notice in this figure two interesting features : a drop in the cross section at $M_H = 2m_W$ due to the opening of the W^+W^- threshold and the peaking of the cross-section for $\frac{4m_{top}^2}{M_H^2} \approx 0.7$

We are now in a position to compare the cross-section for Higgs production as given by eq. (11) with that for the background of process (2) as given by eq.(9). Because the Higgs boson is very narrow below threshold, a meaningful comparison of the signal to the background in this region must take into account the experimental resolution. For conservativeness, we take a resolution $\Delta E = 10\text{ GeV}$. In Figs.4a-d, we show the differential cross section $\frac{d\sigma}{dM}$ as from eq.(9) together with $\frac{\sigma_{H \rightarrow 4\mu}}{\Delta E}$, at the proposed LHC and SSC energy, for two different top mass values, and for both Z_0 's produced with rapidity $|y| \leq 2.5$. We see that the signal is well visible above this particular background. In the figures we have also indicated, with a dashed line, the level expected for the $Z_0^*Z_0^*$ background if process (4) is also included, the latter being estimated to contribute about as much as process (2). This is certainly an overestimate at the LHC, but perhaps an underestimate at the SSC. As for the background due to processes like (3) and (5), they can be eliminated [7] by suitable cuts on the photon invariant mass.

In conclusion, we have shown that the production cross section of the Higgs boson in the 4μ channel for mass values $m_Z \leq M_H \leq 2m_Z$ is well above the background from process (2). Estimates of the background from process (4) and

the use of proper cuts on the mass of the mu-pairs produced through processes (3) and (5) indicate therefore that detection of the Higgs boson depend on the expected experimental resolution and machine luminosity, but not from overwhelming physics backgrounds.

References

1. ALEPH Collaboration, Physics Letters 236, 233 (1990). OPAL Collaboration, Physics Letters 236, 225 (1990).
2. Proceedings of the Workshop on Physics at Future Accelerators, La Thuile , 7-13 January 1987. CERN Scientific Publications, Geneva 1987.
3. CDF Collaboration, F. Abe et al., Physical Review Letters 64, 142 (1990); ibid. 147 (1990).
4. C.Rubbia, 'Future Physics with Accelerators', Proceedings of the European Particle Accelerator Conference, EPAC, June 7-11 1988. Ed. S. Tazzari. Published by World Scientific. Singapore 1989.
5. R.W. Brown and K.O.Michaelian, Physical Review D19 922 (1979) .
E.W.N.Glover and J.J.van der Bij, Nucl. Phys. B321, 561 (1989).
6. J.F.Gunion, P.Kalyniak, M.Soldate and P.Galison, Phys. Rev. D34, 101 (1986).
7. J.F. Gunion, G.L. Kane and J. Wudka, Nuclear Physics B299, 231 (1988).

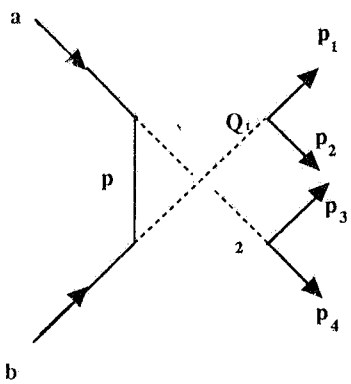
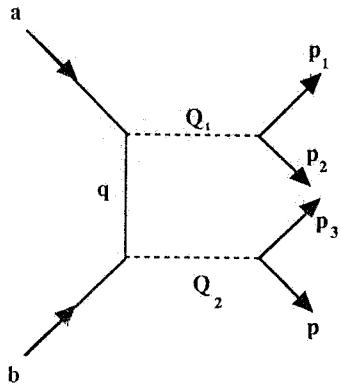


Fig.1 Graphs contributing to the process $q\bar{q} \rightarrow Z_0^*Z_0^* \rightarrow (\mu^+\mu^-)(\mu^+\mu^-)$.

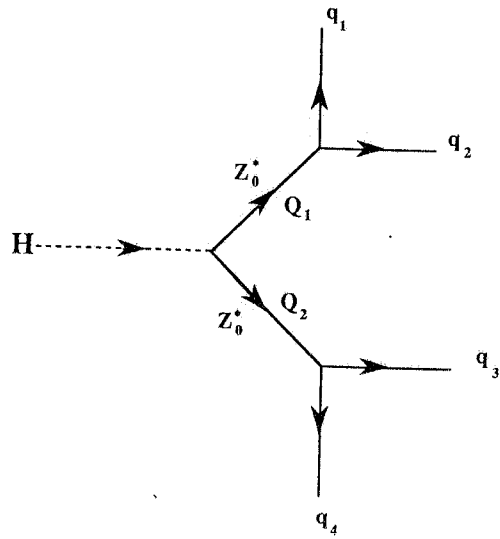


Fig.2 Graph for the process $H \rightarrow Z_0^*Z_0^* \rightarrow (\mu^+\mu^-)(\mu^+\mu^-)$.

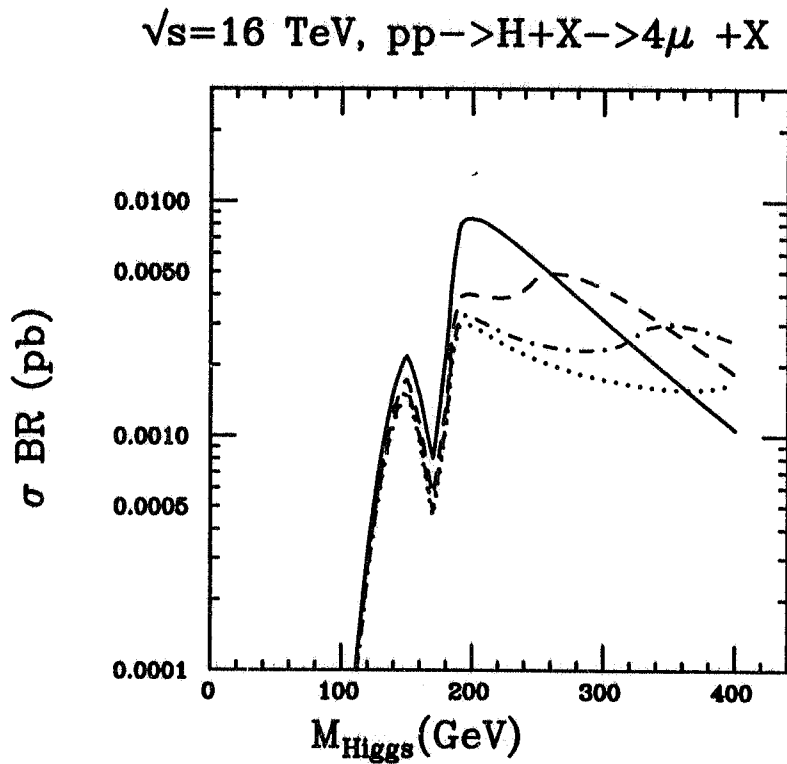


Fig.3 Production cross-section for

$$pp \rightarrow H + X \rightarrow Z_0^* Z_0^* + X \rightarrow (\mu^+ \mu^-)(\mu^+ \mu^-) + X$$

at $\sqrt{s} = 16 \text{ TeV}$. Plots are for $m_{top} = 90 \text{ GeV}$ (full line), $m_{top} = 120 \text{ GeV}$ (dashes), $m_{top} = 160 \text{ GeV}$ (dot-dashes) and $m_{top} = 200 \text{ GeV}$ (dots). The Higgs branching ratio has been calculated for $m_{top} = 90 \text{ GeV}$ for all the curves, since the difference is very small.

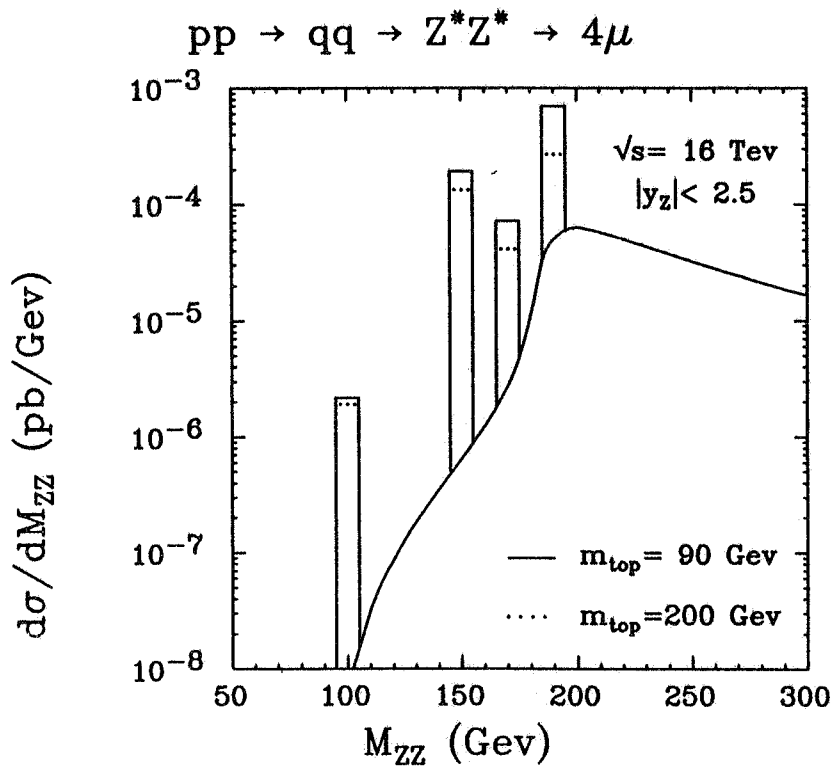


Fig.4a Differential cross section(full line) for the process

$$pp \rightarrow q\bar{q} + X \rightarrow Z_0^*Z_0^* + X \rightarrow (\mu^+\mu^-)(\mu^+\mu^-) + X$$

and the total cross-section per 10 GeV for the process

$$pp \rightarrow H + X \rightarrow Z_0^*Z_0^* + X \rightarrow (\mu^+\mu^-)(\mu^+\mu^-) + X$$

. Curves are for $\sqrt{s} = 16 \text{ TeV}$, $m_{top} = 90 \text{ GeV}$ (full line) and 200 GeV (dots), $|y| \leq 2.5$.

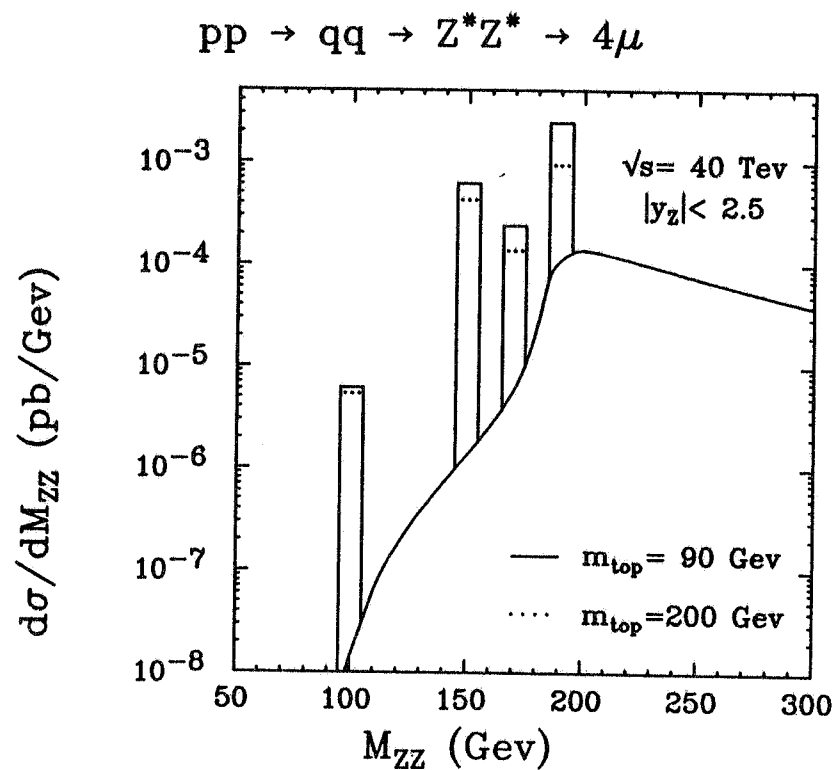


Fig.4b As in Fig.4a with $\sqrt{s} = 40 \text{ TeV}$.